ELSEVIER

Computational Materials Science 17 (2000) 490–495

COMPUTATIONAL MATERIALS SCIENCE

www.elsevier.com/locate/commatsci

Reversal modes and reversal times in submicron sized elements for MRAM applications

T. Schrefl *, J. Fidler

Institute of Applied and Technical Physics, Vienna University of Technology, Wiedner Hauptstraße 8-10, A-1040 Vienna, Austria

Abstract

The switching behavior of submicron sized NiFe nanoelements was calculated using a hybrid finite element/boundary element method. The numerical integration of the Gilbert equation of motion reveals the transient states during magnetization reversal under the influence of a constant applied field. The reversal mode and the reversal time sensitively depend on the size and the shape of the elements. The $200\times100\times10$ nm^3 elements switch well below 1 ns for an applied field of 80 kA/m and a Gilbert damping constant $\alpha = 0.1$. The elements reverse by non-uniform rotation. If an external field is applied the magnetization starts to rotate near the ends, followed by the reversal of the center. This process requires only about 0.1 ns. In what follows, the magnetization component parallel to the field direction shows oscillations, which decay within a time of 0.4 ns. The excitation of spin waves is caused by the precession of the magnetization around the local effective field. A rapid decay of the oscillations is obtained in elements with slanted ends, where surface charges cause a transverse demagnetizing field.

Keywords: Numerical micromagnetics; Fast switching; Spin waves; MRAM

1. Introduction

Patterned magnetic elements used in random access memories (MRAM) and sensor applications require a well defined switching characteristic. The switching speed of magnetic devices has been of interest since the application of magnetic core memories. In a theoretical study, Kikuchi [1] investigated the dependence of the switching time on the Gilbert damping constant α. Solving the Gilbert equation of motion, he derived the critical value of α which minimizes the reversal time. The critical damping occurs for $\alpha = 1$ and $\alpha = 0.01$ for uniform rotation of the magnetization in a sphere and an ultra-thin film, respectively. Recently, experimental measurements as well as numerical micromagnetic simulations [2–4] were applied to analyze the reversal modes and switching times of MRAM memory cells. Russek [2] showed that it is possible to successfully switch pseudo-spin valve memory devices with a line width of 400–800 nm with pulses whose full width at half maximum was 0.5 ns. Gadbois et al. [3] investigated the influence of tapered ends and edge roughness on the switching threshold of memory cells. Koch et al. [4] compared experimental results with micromagnetic simulations of the switching speeds of magnetic tunnel junctions.

This work applies a hybrid finite element/boundary element method [5] to investigate

* Corresponding author. Tel.: +43-1-58801-13729; fax: +43-1-58801-13798.

E-mail address: schrefl@email.tuwien.ac.at (T. Schrefl).

0927-0256/00/$ - see front matter
PII: S0927-0256(00)00075-6

the influence of size and shape on the switching dynamics of submicron thin film NiFe elements. The numerical integration of the Gilbert equation of motion provides the time resolved magnetization patterns during the reversal of elements with flat, rounded, and slanted ends. Section 2 of this paper gives the micromagnetic background and the computational details. Section 3 presents the numerical results, focusing on the reversal modes and spin wave excitations.

2. Micromagnetics and computational details

The simulation of switching dynamics starts from the Gilbert equation of motion [6],

$$\frac{\partial \boldsymbol{J}}{\partial t} = -|\gamma|\boldsymbol{J} \times \boldsymbol{H}_{\text{eff}} + \frac{\alpha}{J_s}\boldsymbol{J} \times \frac{\partial \boldsymbol{J}}{\partial t} \tag{1}$$

which describes the motion of the magnetic polarization vector $\boldsymbol{J}$ in an effective field $\boldsymbol{H}_{\text{eff}}$. The semi-discretization of (1) using a finite element method leads to a system of ordinary differential equations which is integrated using either a Runge–Kutta method or a semi-implicit backward difference scheme depending on the current stiffness of the equations. A hybrid finite element/boundary element method [7] is applied to calculate the demagnetizing field.

A Runge–Kutta method optimized for mildly-stiff differential equations [8] proved to be effective for the simulation using a regular finite element mesh and $\alpha \geqslant 0.2$. However, for an irregular mesh as required for elements with rounded ends and a Gilbert damping constant $\alpha = 0.1$ a time step smaller than 10 fm is required to obtain an accurate solution with the Runge–Kutta method. In this highly stiff regime, backward difference schemes allow much large time steps and thus the required CPU time remains considerably smaller than with the Runge–Kutta method. Fig. 1(a) presents the flow chart of the semi-implicit method for time integration. Since the stiffness arises mainly from the exchange term, the demagnetizing field can be treated explicitly and thus is updated after a time interval τ. During the time interval τ the Gilbert equation is integrated with a fixed demagnetizing field using a higher-order backward difference method. τ is taken as inversely proportional to the maximum torque acting over the finite element mesh. Fig. 1(b) compares the CPU time as a function of the simulated time during the simulation of $200\times100\times10$ nm^3 NiFe element with rounded ends for the different time integration schemes. The semi-implicit scheme requires

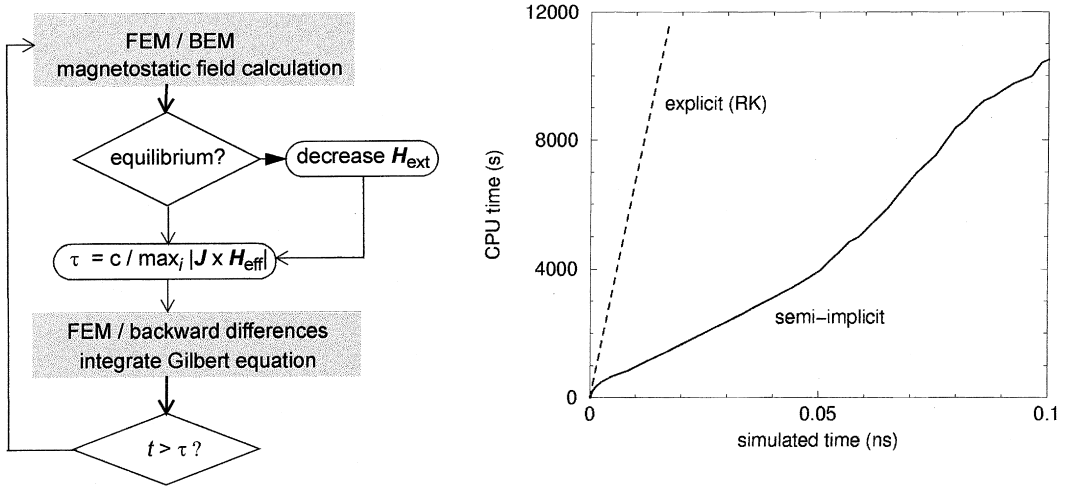

Fig. 1. Flow chart of the semi-implicit time integration scheme and comparison of the CPU time with an explicit Runge–Kutta method.

less CPU time, despite the need to solve a system of nonlinear equations at each time step.

3. Results and discussion

3.1. Particle configurations

Fig. 2 gives the shapes of the NiFe thin films and the finite element mesh used for the calculations. A spontaneous magnetic polarization of $J_s = 1$ T, an exchange constant of $A = 10^{-11}$ J/m and zero magneto-crystalline anisotropy were assumed for the calculations. The extension of the tetrahedron elements was smaller or equal to 5 nm, which corresponds to the exchange length of the material.

3.2. Reversal times

At first the remanent state of the elements was calculated solving the Gilbert equation for zero applied field. The initial state for these calculations was a C like domain pattern. This procedure is believed to provide the minimum energy state for zero applied field. Then a reversed field of $H_{ext} = 80$ kA/m was applied at an angle of 5° with respect to the long axis of the particles.

Fig. 3 gives the time evolution of the magnetization component parallel to the field direction during the switching process for the elements with an extension of $100\times50\times10$ nm^3 and a Gilbert damping constant of $\alpha = 0.2$. In addition Fig. 3 gives the magnetization patterns during the reversal process of the element with rounded ends. Switching occurs by nonuniform rotation of the magnetization. The elements with slanted ends show the fastest switching speed. As compared to the other elements the magnetization remains nearly uniform during the reversal process which reduces the switching time. After the rotation of the magnetization towards the direction of the applied field, the magnetization precesses around the direction of the effective field. As a consequence the magnetization as a function of time shows oscillations.

Fig. 4 presents the time evolution of the magnetization component parallel to the field direction for the elements with rounded and slanted ends with an extension of $200\times100\times10$ nm^3 and a Gilbert damping constant of $\alpha = 0.1$. The comparison of Figs. 3 and 4 clearly shows that the increase in size and the decrease of the damping constant enhances the oscillations of the magnetization after the initial reversal stage. The micromagnetic simulations reveal the following reversal process: at first the magnetization rotates almost in plane towards the direction of the applied field. This process requires only about 0.1 ns. In what follows, the magnetization precesses around the direction of the effective field, which is the sum of the applied field, the demagnetizing field, and the exchange field. The contribution of the demagnetizing field becomes important, whenever the magnetization shows an out of plane component. The precession of the magnetization leads to the excitation of spin waves, which are observed as oscillations of the magnetization component parallel to the applied field direction as a function of time. A lower value of the damping constant

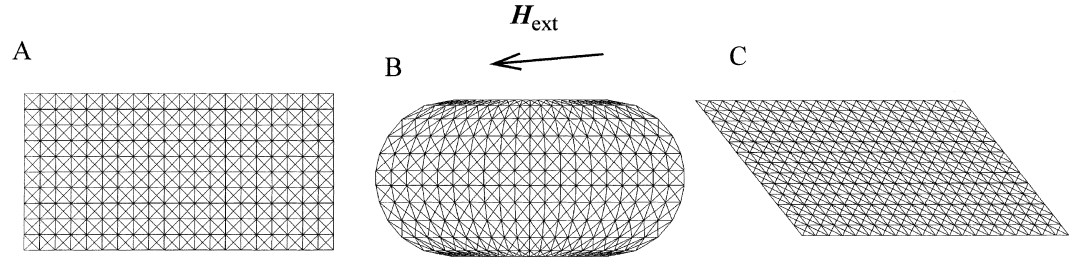

Fig. 2. Top view of the finite element mesh for the elements with flat (A), rounded (B), and slanted (C) ends with an extension of $100\times50\times10$ nm^3. The external field $H_{ext} = 80$ kA/m is applied at an angle of 5°C with respect to the long axis. For the calculations $200\times100\times10$ nm^3 elements, the mesh density was increased as compared to the picture, in order to keep an element size of 5 nm.

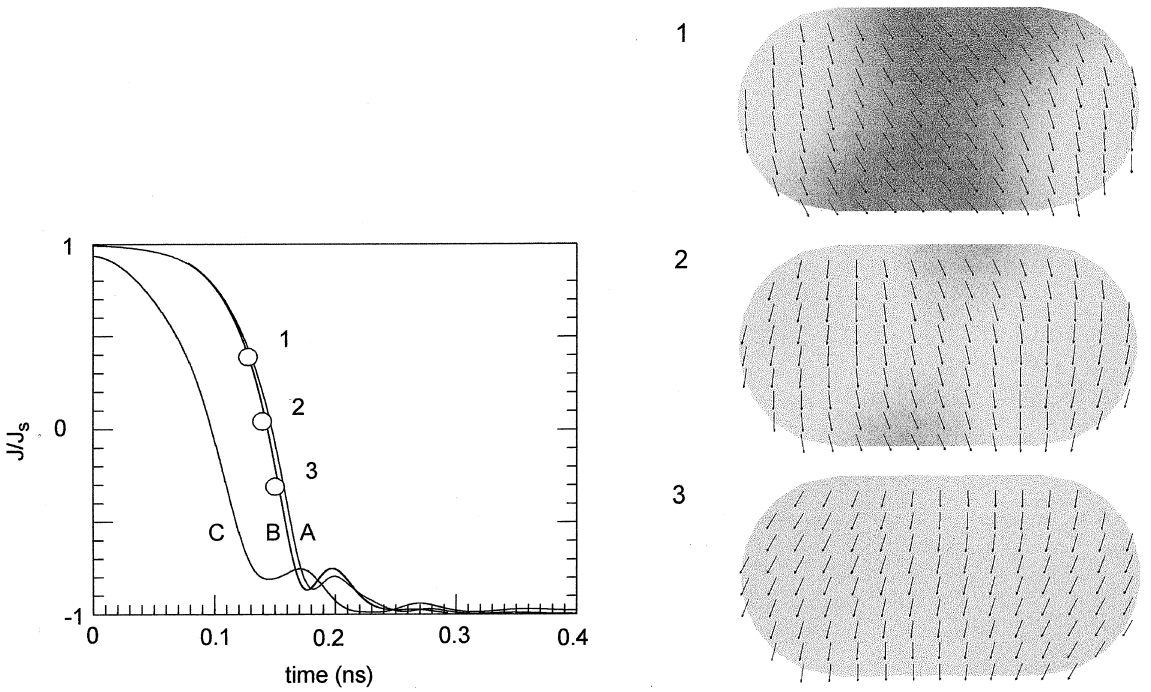

Fig. 3. Left-hand side: time evolution of the magnetization for the elements with flat (A), rounded (B), and slanted (C) ends, an extension of $100\times50\times10$ nm^3 and a Gilbert damping constant of $\alpha = 0.2$. Right-hand side: magnetization patterns during reversal.

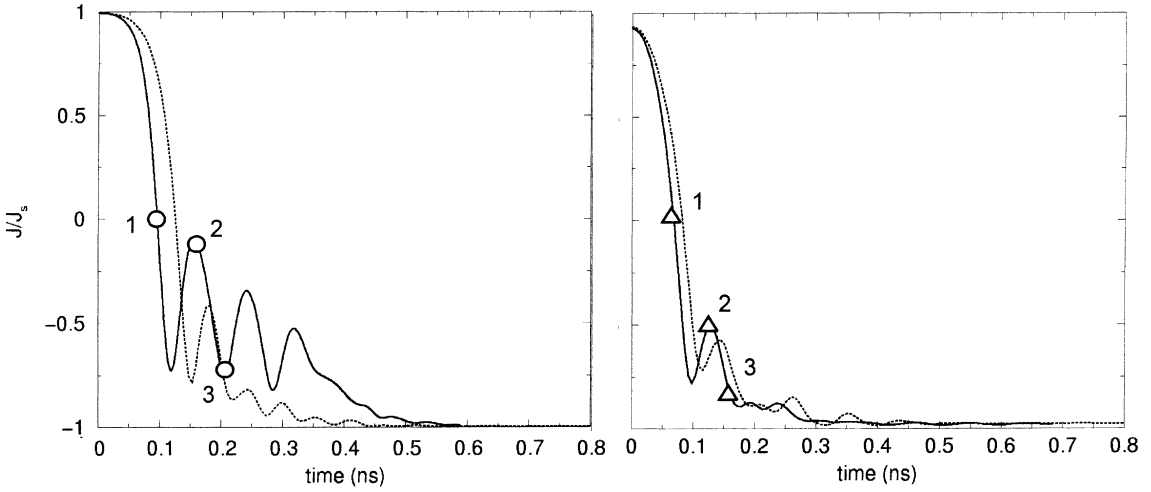

Fig. 4. Time evolution of the magnetization component parallel to the applied field for a Gilbert damping constant $\alpha = 0.1$. Left-hand side: element B (rounded ends), right-hand side: element C (slanted ends). The dotted line and the solid line denote the magnetization as a function of time for elements with an extension of $100\times50\times10$ nm^3 and $200\times100\times10$ nm^3, respectively. The number refers to the magnetization patterns given in Fig. 5.

increases the number of circles the magnetization makes around the effective field. As a consequence the oscillations of the magnetization become more pronounced. The magnetization patterns, given in Fig. 5, clearly show the highly inhomogeneous magnetic states that occur after the initial, in-plane

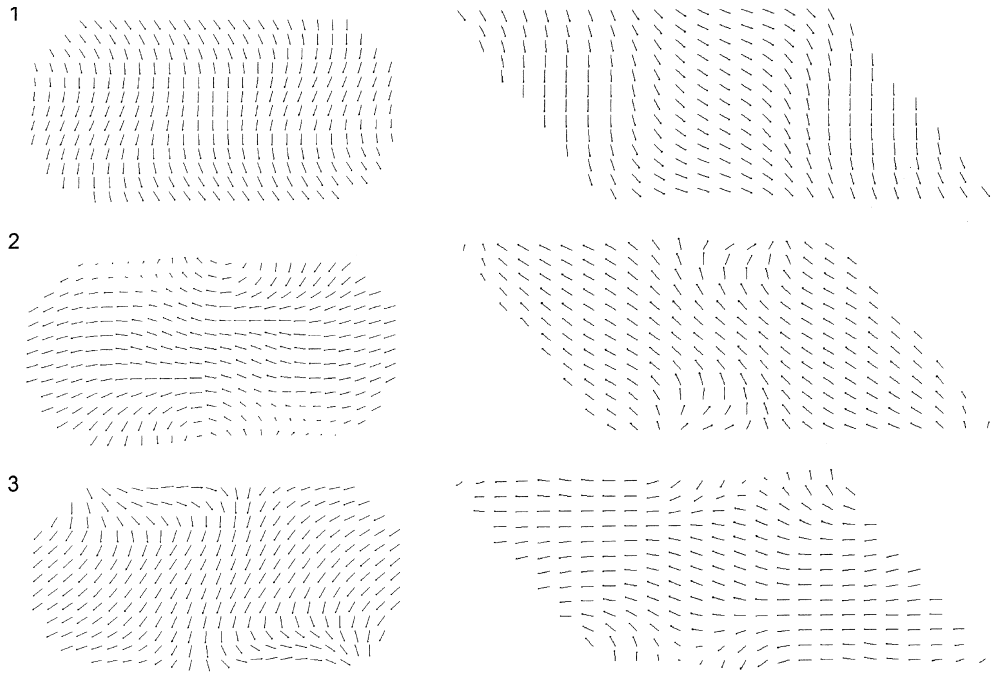

Fig. 5. Magnetization patterns during the switching of the elements with rounded and slanted ends assuming an extension of $200\times100\times10$ nm^3 and a Gilbert damping constant of $\alpha = 0.1$.

rotation of the magnetization. For the elements with rounded ends, the magnetization oscillates several times between the patterns labeled 2 and 3. The oscillations decay within a time of 0.4–0.5 ns. Elements with slanted ends show a smaller amplitude and much faster decay of the oscillations. This effect may be attributed to a transverse demagnetizing field, which arises from surface charges on the tapered ends. This transverse field breaks the symmetry immediately after the initial, in-plane rotation of the magnetization towards the applied field. The oscillations decay within 0.2 ns, reducing the overall reversal time to 0.3 ns.

The time evolution of the micromagnetic energy contributions shows a decrease of the Zeeman energy during the initial, in-plane rotation an energy transfer during the precessional motion of the magnetization. Fig. 6 compares the energies for the elements with rounded and slanted ends, giving the Zeeman energy, the exchange energy, and the magnetostatic energy as a function of time. The plots show that an energy transfer occurs from magnetostatic energy to the exchange and Zeeman energy and vice versa. During the initial rotation of the magnetization, magnetic surface charges at the edges drastically increase the magnetostatic energy. In what follows, a nonuniform state, which reduces the magnetostatic energy is formed. The magnetization changes periodically between highly nonuniform magnetic states with low magnetostatic but high exchange energy and a magnetic state with high magnetostatic energy. Again the comparison of the results show the rapid decay of the oscillations in the element with slanted ends as compared to the element with rounded ends.

4. Conclusions

Micromagnetic finite element simulations show that the shape, size, and the damping constant significantly influence the switching behavior of thin film elements. The magnetization reversal of submicron NiFe elements was found to be a two-stage process. At first, the magnetization rotates almost in plane towards the applied field direction.

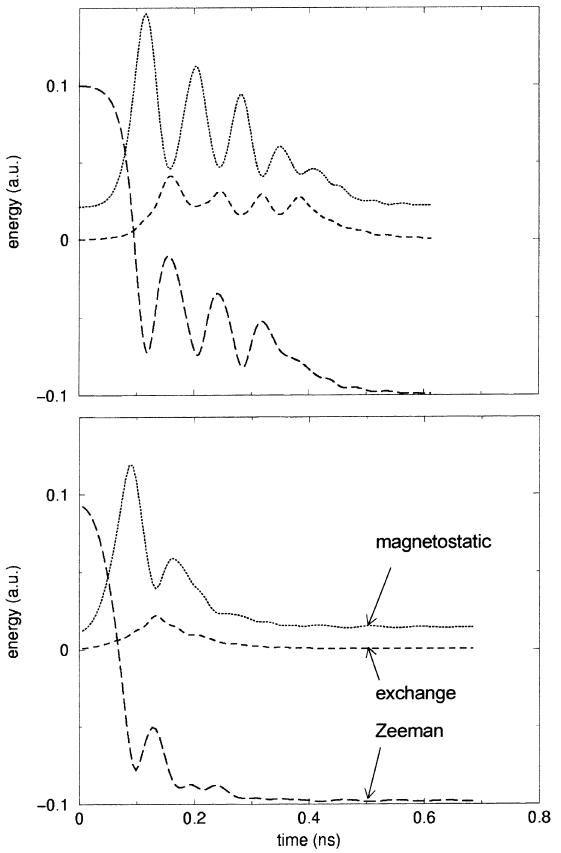

Fig. 6. Micromagnetic energy contributions as a function of time during switching. The dotted, dashed and long-dashed line give the magnetostatic, exchange, and Zeeman energy, respectively. Top: element B (rounded ends), bottom: element C (slanted ends).

In what follows, the precessional motion of the magnetization around the effective field leads to the excitation of spin waves. The time required for the initial rotation of the magnetization decreases with decreasing damping constant and is independent of the element shape. However, the element shape influences the decay rate of the oscillations. A rapid decay is observed in elements with slanted ends. The overall reversal time of $200\times100\times50$ nm^3 NiFe elements is in the range 0.3–0.5 ns.

Acknowledgements

This work was supported by the Austrian Science Fund (P13260-TEC).

References

[1] R. Kikuchi, J. Appl. Phys. 27 (1956) 1352.
[2] S.E. Russek, J.O. Oti, S. Kaka, E.Y. Chen, J. Appl. Phys. 85 (1999) 4773.
[3] J. Gadbois, J.G. Zhu, W. Vavra, A. Hurst, IEEE Trans. Magn. 34 (1998) 1066.
[4] R.H. Koch, J.G. Deak, et al., Phys. Rev. Lett. 81 (1998).
[5] T. Schrefl, J. Fidler, K.J. Kirk, J.N. Chapman, IEEE Trans. Magn. 33 (1997) 4182.
[6] T.L. Gilbert, Phys. Rev. 100 (1955) 1243.
[7] D.R. Fredkin, T.R. Koehler, IEEE Trans. Magn. 26 (1990) 415.
[8] B.P. Sommeijer, L.F. Shampine, J.G. Verwer, Technical Report MAS-R9715, CWI, Amsterdam, 1997.